Journal of Nuclear Materials 401 (2010) 71–77

Contents lists available at ScienceDirect

Journal of Nuclear Materials

journal homepage: www.elsevier.com/locate/jnucmat

Crack initiation and propagation in pile grade A (PGA) reactor core graphite under a range of loading conditions

P.J. Heard [a,*], M.R. Wootton [b], R. Moskovic [b], P.E.J. Flewitt [a,b,c]

[a] Interface Analysis Centre, University of Bristol, Bristol BS2 8BS, UK
[b] Magnox North Ltd, Oldbury Technology Centre, Oldbury Naite, Oldbury-on-Severn, South Gloucestershire BS35 1RQ, UK
[c] HH Wills Laboratory, Dept. of Physics, University of Bristol, Bristol BS8 1TL, UK

ARTICLE INFO

Article history:
Received 24 November 2009
Accepted 26 March 2010

ABSTRACT

The pile grade A (PGA) graphite used in UK gas cooled reactors is a multiphase, polygranular, aggregate material with complex cracking behaviour. Virgin, un-irradiated graphite cylinders 12 mm in diameter and 6 mm long have been subjected to controlled cracking either by insertion of a needle into the material or by compressive loading. The resultant cracking was observed using optical and focused ion beam microscopy. Micro-cracking was confirmed to precede macro-crack formation and this mechanism is consistent with the observed non-linearity in the load–displacement curve prior to peak load. Macro-cracks followed an irregular path controlled by the direction of the applied tensile stress and the microstructure, in particular porosity and filler particles. The results are discussed with respect to the quasi-brittle fracture characteristics of such an aggregate material.

1. Introduction

The manufacture of the graphite moderator bricks used in UK gas cooled reactors has been described elsewhere [1,2]. The pile grade A (PGA) graphite bricks used for the Magnox reactor cores were formed by extrusion. The microstructure of the resulting graphite is a polygranular, aggregate material which consists of three phases. The first phase consists of relatively large graphitised particles, filler, in the size range 0.10–1.0 mm and these are dispersed in a matrix of fine calcined filler particles, below ~10 μm, and graphitised pitch binder. The third phase is porosity, arising from gas evolution, accommodation cracking due to thermal strains, and shrinkage which results from both baking and graphitisation during the manufacture of the bricks [2]. The filler particles formed from needle coke have a needle-like morphology and align with the direction of extrusion, namely the axis of the bricks. Porosity is observed within both the large filler particles and the matrix. Complex interconnected pathways have been observed to link many of these pores throughout the microstructure. Porosity remains, after production, at about 20% comprising both open and closed pores. The closed pores are generally associated with the filler particles and result from shrinkage during the calcination and graphitisation stage of manufacturing. By comparison open pores are contained mainly within the matrix regions and arise from gas evolution [2–6]. Variation in mechanical and physical properties, and microstructure are observed between different bricks and within the same brick, but these were limited by applying strict quality procedures at the time of manufacture [2,12].

In a previous review it was proposed that the porous reactor core graphite used for the manufacture of moderator bricks has quasi-brittle fracture characteristics [1]. It was recognised that these graphites are multiphase, polygranular, aggregate materials and as such have a microstructure with features similar to other aggregate materials such as concrete [7–11]. The non-linear load–displacement (stress–strain) response arising from the presence of distributed micro-cracks leading to the final failure is representative of quasi-brittle fracture [1,11]. A typical example is shown by the load–displacement response for bend geometry specimens (Fig. 1). It is recognised that there is no evidence that polygranular, aggregate graphites can be plastically deformed. Hence, the change in compliance together with any deviation from an initial linear shape of the load–displacement curve can be attributed to micro-cracking. The compliance at any point during the test is equal to displacement divided by the load. Fig. 1 shows that after an initial linear response which is proportional to the Young modulus of elasticity, region I, there is a non- linear, rising portion of the load–displacement curve, region II, prior to the peak load caused by the development of distributed, stable micro-cracks. Post peak load, in region III, the micro-cracks coalesce into branched macro-cracks. This is then often accompanied by post peak softening. Unloading laboratory bend specimens in the rising load–displacement curve prior to peak load, when the curve is non-linear, follows a linear path with a slope inversely

* Corresponding author. Tel.: +44 117 3311175; fax: +44 117 9255646.
E-mail address: Peter.heard@bristol.ac.uk (P.J. Heard).

0022-3115/$ - see front matter Crown Copyright © 2010 Published by Elsevier B.V. All rights reserved.
doi:10.1016/j.jnucmat.2010.03.023

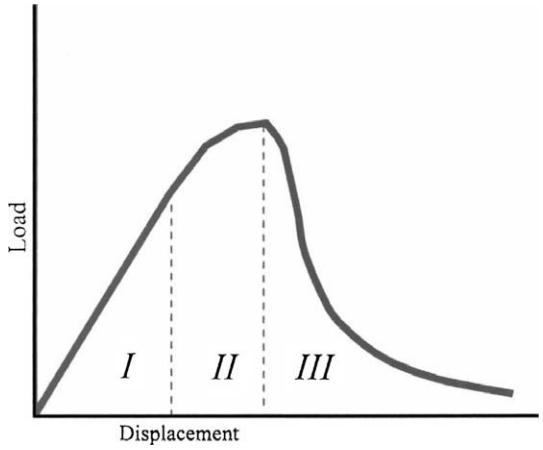

Fig. 1. A characteristic bend geometry load–displacement curve for a quasi-brittle material, region I is linear, region II is non-linear, region III is post peak softening.

proportional to the compliance. It has been shown that linear elastic fracture theories do not apply to quasi-brittle materials and hence are not appropriate to reactor core graphite [9].

As-formed graphite has a crystal structure that is layered and the atoms can be stacked in three different high symmetry ways. These are usually labelled AA, AB and ABC graphite according to the different relative translations of the layers. The AB form is by far the most abundant and AA is recognised to be unstable. The AB graphite has an orthorhombic structure (pseudo-hexagonal) that consists of layers of hexagonal carbon atom rings that form the basal planes [13–15]. While the atoms in each layer have covalent bonds [9,12], the presence of weaker bonds between the basal planes provides low energy pathways for cleavage fracture [13,14]. It is well established that polygranular reactor core graphites are subject to brittle fracture [6–8]. The needle-like filler particles in PGA graphites become aligned during extrusion so that mechanical and fracture properties are different in the axial and transverse directions. The graphite microstructure and therefore the mechanical and physical properties change over the service life of the reactors due to two processes: (i) neutron irradiation which introduces point defects into the crystal lattice that increase the strength as a function of the irradiation dose and temperature [3,14] and (ii) radiolytic oxidation by CO_2 gas, from the gamma-irradiation produced by nuclear fission, which causes material mass loss and a decrease in the strength. The effect of the radiolytic oxidation is to: (i) decrease the density of the material, (ii) increase pore size, (iii) increase connectivity, (iv) decrease inter-pore spacing and (v) modify the distribution of the pores between filler and binder.

Novel computer-based imaging techniques combined with image processing technologies offer powerful methods for evaluating the microstructure of materials such as graphite. Indeed, the pore structure of un-irradiated and to a lesser extent irradiated PGA graphite has been examined by X-ray tomography and to a higher spatial resolution using focused ion beam serial sectioning combined with 3-D image reconstruction [16,17]. The latter shows, in particular, the complex interconnectivity of the pores. Moreover these pores and interconnecting paths can have sizes spanning the nano- to milli-metre scale range. In addition, techniques have been developed to fracture small test specimens using a range of different loading techniques that can be applied to un-irradiated and, if required, irradiated PGA graphite, and highly porous filter graphites [18,19]. The latter can be used as a surrogate for radiolytically oxidised graphite to consider the role of increasing porosity on the load–displacement response and fracture resistance.

In this paper in Section 2 we describe various small specimen test methods used to investigate the initiation and propagation of cracks in PGA reactor core graphite at the micro-scale under various loading conditions. These produced characterized fracture specimens that were examined in a focused ion beam workstation. This allowed these specimens to be subjected to a combination of ion milling including serial sectioning and imaging. The results are described in Section 3 and discussed in Section 4 in the context of the quasi-brittle behaviour of PGA graphite. Conclusions are presented in Section 5.

2. Experimental

2.1. Materials

Cylindrical PGA test specimens were made by trepanning 12 mm diameter rods from bulk PGA graphite and these were sliced into 6 mm thick cylinders using a South Bay Technology Inc. Model 650 low speed diamond wheel saw with deionised water as coolant. The diamond saw produced smooth high-quality surfaces suitable for subsequent microscopic examination. The brick extrusion direction was diametrically across the flat surfaces of the cut cylinders. The extrusion direction was marked on the edges of the cylinders for reference during compression testing.

2.2. Test methods

Controlled cracking was introduced in the graphite specimens by needle insertion or diametral compression loading methods on the cylindrical test specimens. Each method allowed specimens to be subsequently examined under load.

Needle insertion was effected by controlled forced insertion of a needle into the centre of the graphite specimen along the axis of the cylinder. Specimens were supported within a cylindrical holder so that the top surface of the graphite could be observed under an optical microscope while a needle was progressively forced

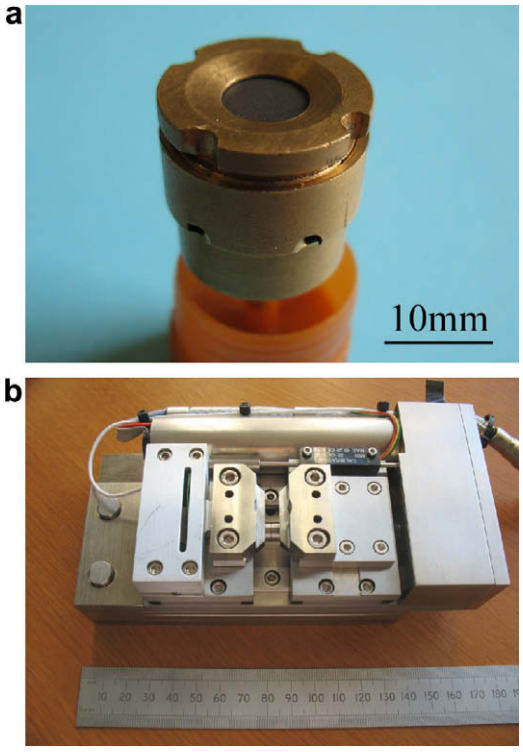

Fig. 2. Micro-scale mechanical testing methods: (a) needle insertion method showing specimen holder and (b) compression tester.

through the specimen from underneath, Fig. 2a. A stainless steel needle, with a shank diameter of 0.65 mm and a tip radius of approximately 30 μm was used. The needle was mounted in M3 brass studding for controlled insertion into the specimen. The movement of the needle through the thickness of the specimen was monitored by counting the number of turns of the screw M3 thread (pitch of 0.5 mm). The needle was gradually pushed into the specimen until it was approximately 2–3 mm below the upper surface of the cylinder. This generated a tensile stress field in the graphite ahead of the needle and gave rise to cracking. Movement of the needle was stopped when fine cracks were observed optically on the upper surface of the specimen thus avoiding uplifting of material. This facilitated observation of the early stages of cracking by optical microscopy, or focused ion beam imaging, as detailed below, without retracting the needle, so that load was maintained and cracks remained open.

Compression testing of the cylindrical specimens was done using a Deben compression/tensile stage (MicroTest 2000 model, Gatan Ltd., Abingdon, Oxon, UK). The unit is capable of operation on the desk or within a scanning electron microscope or focused ion beam workstation. A photograph of the unit is presented in Fig. 2b. The stage can be operated at compression speeds of between 0.033 and 0.4 mm/min, with a load cell giving force measurements up to a maximum of 2 kN. The cylindrical graphite specimens were loaded into the compression tester such that the direction of the compressive load was along a diameter of the flat face of the cylinders, chosen here to be the extrusion direction of the graphite. This provided a tensile load normal to the direction of the applied load so that cracks would be induced in the plane parallel to the load direction. As compression was along the diameter of a cylindrical specimen, anvils with a small arc and curvature equal to that of the specimen were used to distribute the load more evenly. Load–displacement curves were recorded whilst observing the surface of the specimen by optical microscopy or focused ion beam.

2.3. Characterization methods

An Olympus SZ11 low power binocular microscope fitted with a DeltaPix InfinityX camera (Kane Computing, Northwich, Cheshire, UK) was used for the acquisition of optical images of the graphite during both needle insertion and compression testing. A ring-shaped light source was used to illuminate the specimens to avoid the formation of bright spots in the image arising from specular reflection from smooth features which would accompany spot illumination. The resulting illumination facilitated the detection of small cracks formed as a result of progressive loading.

Precision milling and high-resolution imaging of surface and sub-surface features in the graphite was carried out using an FEI Strata FIB-201 focused ion beam (FIB) workstation [20]. The instrument was used to mill trenches into the graphite by sputtering with the gallium ion beam, producing high-quality vertical sections through the material to depths of approximately 20 μm. The gallium ion energy was 30 keV with the beam current adjusted according to milling and imaging requirements. Trenches were cut into the material at higher beam currents, starting at 12 nA and reducing to about 1 nA, initially producing a staircase-shaped trench and then cutting using a line scan. During the etching process, water vapour at low pressure was introduced into the work chamber, both to enhance the cutting speed and more significantly to prevent redeposition of material. A good quality surface for imaging was produced by scanning the ion beam with an ion current of about 1 nA in a line and moving the beam gradually into the deepest face. The sample was then tilted to 45° to image the cut face at beam currents of 11 pA or less and thus obtain images at high resolution.

3. Results

3.1. Material microstructure

PGA graphite has a complex structure of filler particles interspersed with matrix material which consists of small flour particles and the graphitised residue of the pitch used in the production of the initial extruded green brick and the subsequent impregnation to increase the brick's density. When examined at high resolution in the FIB, the two areas have very distinct microstructures. Filler particles (Fig. 3 left hand side) are solid with isolated shrinkage (Mrozowski) cracks. The matrix areas (Fig. 3 right hand side) are dominated by the presence of lamellar graphite. This is believed to be the graphite residue of the mesophase produced during the graphitisation of the pitch. Serial sections of the region shown in Fig. 3 and in other similar areas reveal that the porosity in such regions is interconnected.

3.2. Load–displacement

The load–displacement curve resulting from compression of a cylindrical PGA specimen is shown in Fig. 4. Compression proceeded at a rate of 0.1 mm/min. Displacement and load measurements were recorded at 500 ms intervals. The initial region, up to 0.1 mm displacement, had a relatively low slope, characteristic of a "bedding-in" region in which the specimen accommodated to the compression clamps. A linear region was observed between 0.2 and 0.3 mm displacement, in which elastic deformation occurred. Beyond this point the curve became non-linear with a gradually reducing compliance, until peak load was reached. After the

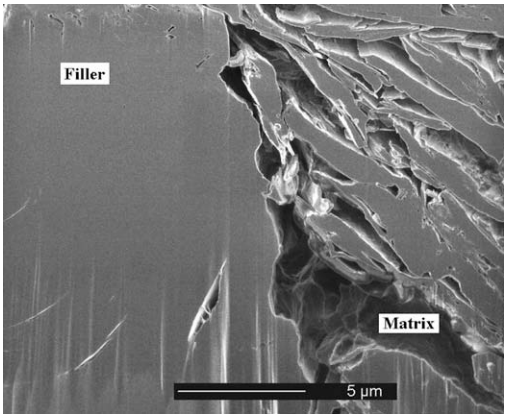

Fig. 3. Microstructure of virgin PGA graphite revealed by FIB sectioning and imaging.

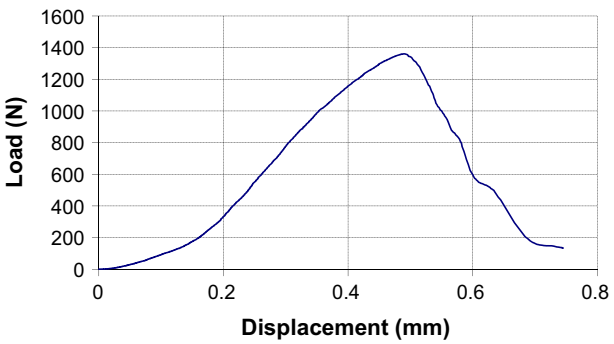

Fig. 4. Load–displacement curve from compression of a cylindrical PGA specimen.

load maximum, failure was gradual with force reducing slowly with displacement.

3.3. Microstructure/fractography of crack initiation and propagation

3.3.1. Needle insertion

The needle insertion method was used on a PGA graphite specimen and the top surface was monitored optically until very fine cracking was observed. The specimen was then transferred to the FIB for high-resolution surface and sub-surface microscopy.

Fig. 5 shows FIB images of a region in which some cracking had been detected optically. Trenches were milled into the specimen using the FIB to produce vertical faces 1 and 2, which are separated by about 3 μm as shown in Fig. 5a. FIB images of the faces (produced by tilting to 45°) are shown in Fig. 5b and c. Here a large sub-surface crack has formed within a filler particle. The regions either side of the crack appear to be dense and relatively free of cracks. To the right of the main crack, marked by the arrows, is a region of dispersed, fine micro-cracking. This feature is present in both face 1 and 2 together with some dispersed damage. Features such as this are not observed in PGA graphite prior to loading.

3.3.2. Compression

The compression method was used on a PGA graphite specimen, monitoring the top face of the graphite optically and compressing across a diameter of the specimen in the extrusion direction. A compression rate of 0.1 mm/min was again used. The load–displacement characteristics were recorded at 500 ms intervals and optical images were recorded at 1s intervals. The optical images obtained at the start of the process and at 0.55 mm displacement (beyond peak load) are shown in Fig. 6a and b respectively. Cracking appear to have occurred mainly within the matrix and pass around the filler particles.

The compression method was used on a PGA graphite specimen within the FIB system. Compression proceeded until fine cracking was observed at the top surface of the sample in the FIB. Sites were then chosen for FIB trenching, generally at positions across the observed cracks close to the crack tip, or ahead of the crack tip. The sample was then tilted to 45° for high-resolution imaging of the cut face to observe sub-surface detail. Compression was resumed, increasing the load by small increments, realigning the sample to centre the region of interest in the field of view and recording images. Force increments of 40 N were used and FIB images were captured at 8000× magnification, giving a horizontal field of view of 38 μm. Fig. 7 shows FIB images of the cut face of the specimen at compression loads of: (a) 497 N, (b) 560 N and (c) 830 N respectively. The arrows in Fig. 7b and c mark the position of a crack forming and developing in the bulk of the graphite, within a filler particle. After crack formation, the two halves slide across each other. Other features within the sample, for example those on the right hand side of the face, appear to exhibit elastic deformation.

FIB images of a second PGA specimen under compression testing are shown in Fig. 8. Fig. 8a corresponds to a loading of 740 N. Fig. 8b shows the same region after the load had been increased to 980 N. A vertical crack is observed to have opened, with material at either side of the crack moving in a shear motion. Fine cracking is observed around the region of the main crack, which may be distributed damage.

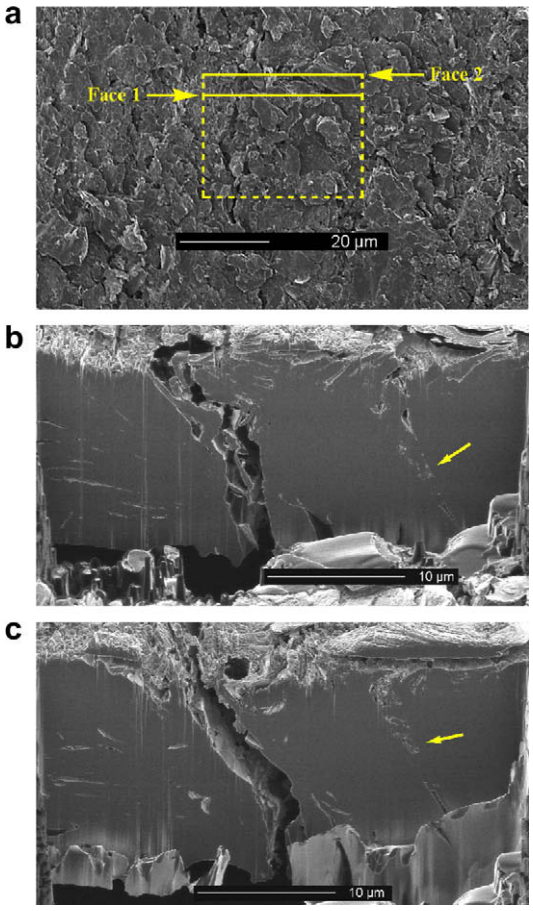

Fig. 5. PGA specimen after needle insertion: (a) surface with positions of FIB trenches marked, (b) face 1 of milled region and (c) face 2 of milled region.

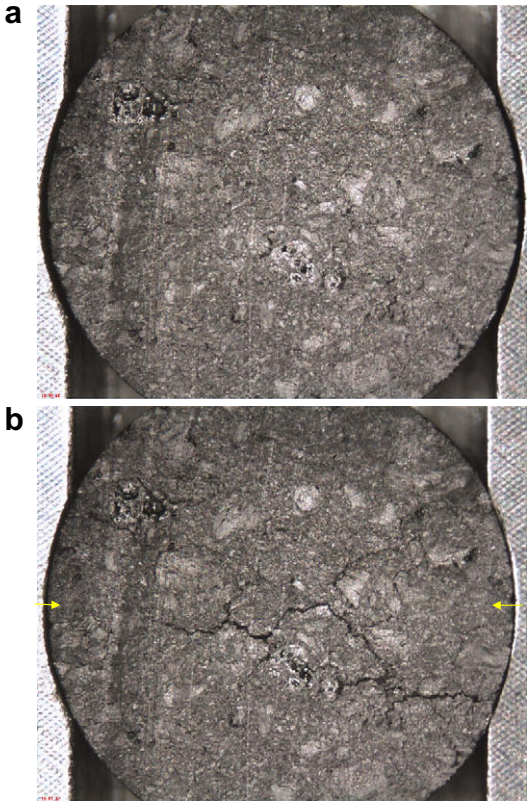

Fig. 6. Optical image of PGA specimen: (a) before compression and (b) after 0.55 mm compressive displacement showing macro-cracking (displacement is horizontal, as shown by arrows).

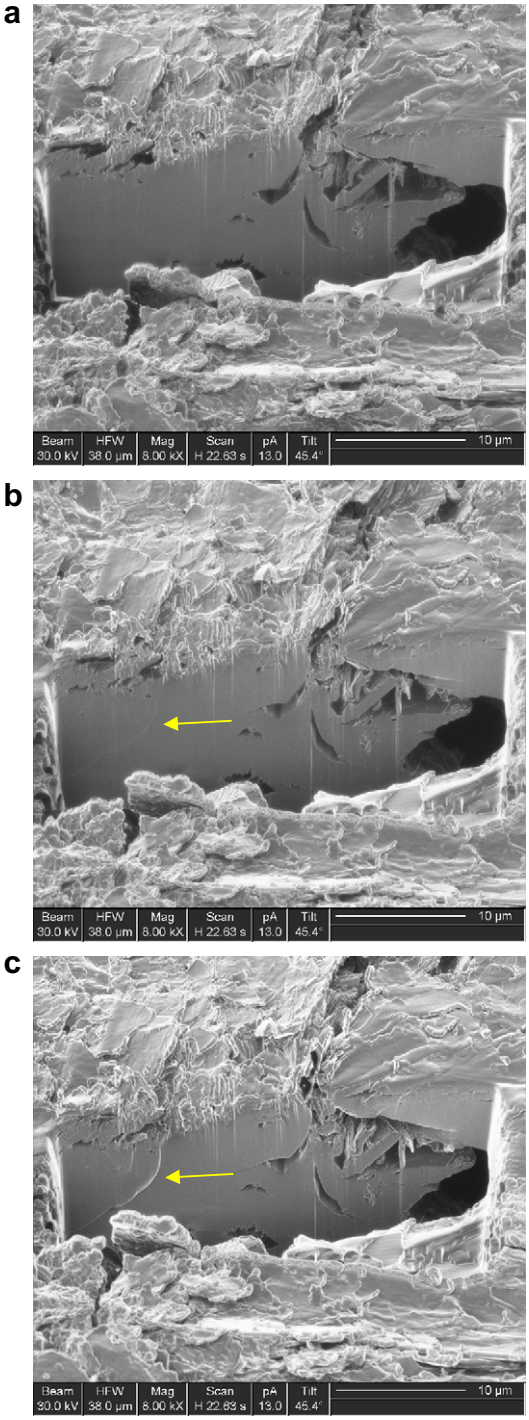

Fig. 7. FIB images of PGA specimen under (a) 497 N, (b) 560 N and (c) 830 N compression. Arrows show developing micro-crack.

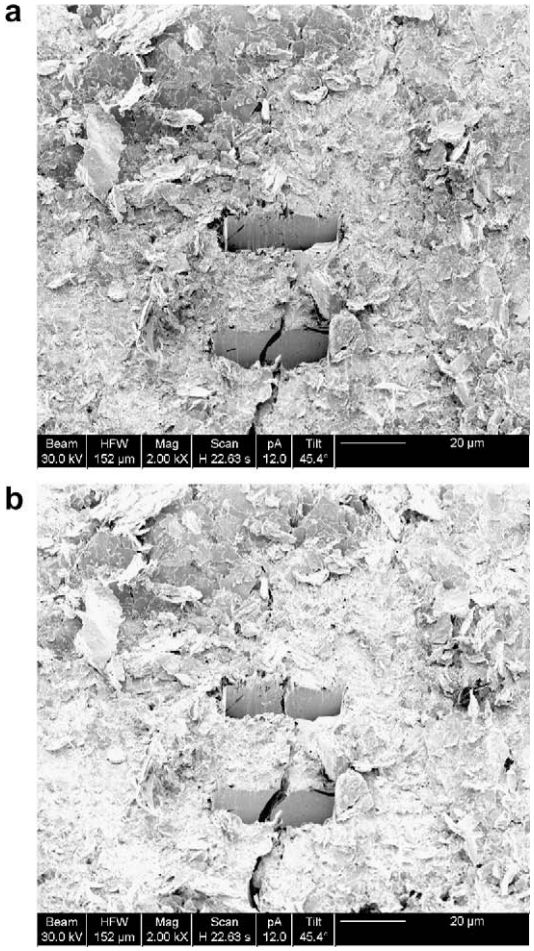

Fig. 8. FIB images of second PGA specimen under: (a) 740 N compression and (b) 980 N compression where the initially arrested micro-crack has extended.

4. Discussion

Despite the widespread use of polygranular graphite for the construction of the gas cooled reactor cores in the UK reactor plant, there remain issues relating to the detailed understanding of the fracture processes at the micro-scale. In general, within the industry plain section beam specimens of both un-irradiated and irradiated graphite are tested to provide a measure of the fracture strength of the material and the variation with weight loss [1]. A typical load–displacement curve obtained for PGA graphite is shown in Fig. 9a. Following a linear change with load there is a non-linear increase prior to achieving peak load and then a decrease beyond the maximum which is, in part, progressive [1]. It

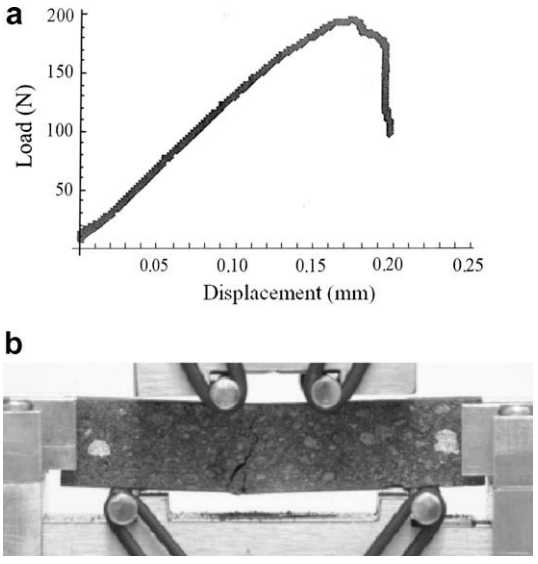

Fig. 9. Four-point bend testing of an un-irradiated PGA graphite specimen: (a) load –displacement curve and (b) Fracture specimen in the four-point bend test rig.

is noteworthy that there is significant variability in the shape of the non-linearity prior to peak load and also post peak load from specimen to specimen. This is a direct consequence of heterogeneity in the microstructure of the polygranular graphite relative to the size of the specimens tested [1]. As shown in Fig. 9b the final macro-crack path is irregular and related to the direction of the applied tensile strain and the microstructure of the graphite.

In this paper we have adopted two novel test procedures to load graphite specimens combined with high-resolution imaging to investigate further the micro-cracking pre-peak load and macro-cracking post peak load with respect to the microstructure of un-irradiated PGA graphite. Both the needle insertion and the disc compression test methods, Fig. 2a and b, provide the capability to view the surface of the small disc specimens when subject to a given load and under a progressively increasing applied load. The former is important since, when using X-ray tomographic imaging of loaded and cracked, notched compact geometry un-irradiated Gilsocarbon graphite specimens, Hodgkins [21] and Hodgkins et al. [22] have observed closure of both the micro-and macro-cracks when the load is removed. This makes examination of cracking extremely difficult even when using high-resolution imaging techniques, for example focused ion beam imaging, unless a load is applied. The use of ion beam milling to produce surfaces normal to the specimen surface has provided the opportunity, for both test methods, to correlate surface and sub-surface microstructure and crack morphology. Fig. 3 provides a measure of the quality of such a milled surface in un-irradiated graphite. Here the large filler particle contains small closed pores and a range of small ($\leqslant$2 μm long) Mrozowski cracks arising from thermal shrinkage which occurs during manufacture of the graphite [4,5]. The porous region immediately to the right of the filler particle demonstrates the complex geometry of pores arising from gas evolution and shrinkage within the matrix.

The load–displacement curve, Fig. 4, obtained for the compression disc test shows initial "bedding" of the specimen to a load of about 300 N. There follows a short linear range where the material behaves elastically, prior to the onset of non-linearity. The ion milled section sequence, Fig. 7, shows that as the load is increased from 497 N, (Fig. 7a), to 560 N, (Fig. 7b), a micro-crack is formed and the feature becomes enhanced when the load has reached 830 N, (Fig. 7c). This sequence provides evidence that micro-cracks initiate and propagate prior to peak load to accommodate specimen displacement. This is supported by the sequence in Fig. 8 where a second slot has been milled ahead of the micro-crack in Fig. 8a. Increasing the load from 740 N to 980 N has resulted in the arrested micro-crack extending under further loading across the second slot, (Fig. 8b). Therefore from a load of about a third of the peak load to the peak load, micro-cracks have been found in the compressed disc aligned broadly parallel to the direction of the applied stress. This micro-cracking accommodates a displacement of ~0.35 mm.

At peak load and beyond, micro-cracks link to form the dominant macro-cracks shown in Figs. 5 and 6 for specimens loaded by both needle insertion and disc compression. Moreover Fig. 5 provides limited evidence for micro-cracking on the flank of a macro-crack. When interrupted post peak load, Fig. 6 shows that the macro-cracks follow an irregular path similar to that observed previously in the flexural test specimens of fractured un-irradiated PGA graphite (Fig. 9b). The macro-cracks follow a path dominated by the direction of the applied tensile stress and the microstructure. In particular the cracks tend to link regions of porosity and filler particles. Although in some cases these cracks traverse suitably oriented filler particles, in general they propagate along the weaker particle–matrix interface. Transgranular fracture will occur within the particles only on those occasions when the resolved traction stress across the basal plane is greater than that occurring at the particle–matrix interface [13,14]. This is consistent with the conclusions of several workers [1,23] who link overall fracture strength of polygranular graphites with the strength of this interface.

The results from these observations of cracking on a micro-scale are consistent with views presented by Hodgkins et al. [1] that un-irradiated polygranular reactor core graphites deform and fracture in a brittle mode consistent with quasi-brittle behaviour encountered in a range of porous aggregate-containing materials [1,9–11]. Micro-cracks initiate and propagate to accommodate displacements prior to the initiation of a macro-crack or cracks. Indeed, a distribution of micro-cracks which develop prior to peak load arrest as the local stress is accommodated. The fracture path of the macro-cracks initially links micro-cracks and is controlled by the direction of the applied tensile stress and the polygranular aggregate microstructure. The filler particle–matrix interface is important in defining the overall strength and fracture path. Hence, PGA un-irradiated graphite has characteristics of quasi-brittle fracture commensurate with other aggregate-containing porous materials such as concretes and mortars.

5. Conclusions

It may be concluded from this micro-scale investigation that:

(i) Both the needle insertion and the diametral compression of small, 12 mm dia. × 6 mm, disc specimens provides a useful tool for examining crack formation in polygranular reactor core graphite, particularly when supported by focused ion beam milling and imaging.
(ii) Micro-cracks in un-irradiated PGA graphite have been confirmed to precede macro-crack formation. The micro-cracking accommodates the non-linearity in the load–displacement curves prior to the peak load. Such cracks have been observed at loads which are as low as 30% of the peak load.
(iii) Macro-cracks initiate by linking micro-cracks and follow an irregular path controlled by the direction of the applied tensile stress and the microstructure, in particular porosity and the filler particles.

Acknowledgement

This paper is published with the permission of Magnox North Ltd.

References

[1] A. Hodgkins, T.J. Marrow, M.R. Wootton, R. Moskovic, P.E.J. Flewitt, Mater. Sci. Technol., in press, doi:10.1179/026708309x12526555493477.
[2] Nuclear Graphite Production, Nucl. Eng. 175–178, April 1957.
[3] J.V. Best, W.J. Stephen, A.J. Wickman, Prog. Nucl. Energy 16 (1985) 127–178.
[4] S. Mrozowski, Phys. Rev. 86 (1952) 251.
[5] S. Mrozowski, Mechanical strength, thermal expansion and structure of cokes and carbons, in: Proceedings of the 1st and 2nd, Conference on Carbon, 31–45, 1956.
[6] K. Wen, T.J. Marrow, B. Marsden, J. Nucl. Mater. 381 (2008) 199–203.
[7] A.H. Yaghi, T.H. Hyde, A.A. Becker, G. Walker, The Integrity of Graphite Blocks in Nuclear Reactors, University of Nottingham Report, GRA/AHY/040806, August 2004.
[8] B.T. Kelly, Physics of Graphite, Applied Science, London, 1981.
[9] B.L. Karihaloo, Fracture Mechanics and Structural Concrete, Longmans Scientific and Technical, Harrow, 1995.
[10] E. Schlangen, E.J. Garboczi, Eng. Fract. Mech. 57 (1997) 319–332.
[11] E. Schlangen, Key Eng. Mater. 699 (2008) 385–387.
[12] S. Fazluddin, Crack Growth Resistance in Nuclear Graphite, PhD Thesis, University of Leeds, UK, 2002.
[13] C.L. Mantell, Carbon and Graphite Handbook, vol. 9, John Wiley, New York, 1968.
[14] J. Brocklehurst, Chem. Phys. Carbon 13 (1977) 145–279.
[15] A.R. Ubbelohde, F.A. Lewis, Graphite and its Crystal Compounds, Clarenden Press, Oxford, 1960.

[16] C. Berne, S.L. Fok, B.J. Marsden, L. Babout, A. Hodgkins, T.J. Marrow, P.M. Mummery, J. Nucl. Mater. 352 (2006) 1.
[17] G.M. Hughes, P.J. Heard, M.R. Wootton, University of Bristol Report, GMH/IAC/06/07/C01, September 2008.
[18] P.J. Heard, K.R. Hallam, P.E.J. Flewitt, S. Nakhodchi, M. Lamb, M.R. Wootton, University of Bristol Report PJH/IAC/06/08/C01, June 2008.
[19] P.J. Heard, R. Moskovic, M.R. Wootton, University of Bristol Report PJH/IAC/03/09/C02, March 2009.
[20] FEI Europe, Eindhoven, The Netherlands.
[21] A. Hodgkins, Crack Propagation in Nuclear Graphite, PhD Thesis, University of Manchester, 2006.
[22] A. Hodgkins, T.J. Marrow, P. Mummery, B. Marsden, A. Fok, J. Mater. Sci. Technol. 22 (2006) 1045–1051.
[23] J.W. Patrick, A. Walker, Fractographic studies of carbon, Institute of Physics Series, vol. 78, IoP Publishing, Bristol, 1985, pp. 565–568.